Séminaire Équations aux dérivées partielles - École Polytechnique

Vicent Caselles

Bartomeu Coll

Jean-Michel Morel

Partial differential equations and image smoothing

EQUATIONS AUX DERIVEES PARTIELLES

PARTIAL DIFFERENTIAL EQUATIONS
AND IMAGE SMOOTHING

V. CASELLES, B. COLL and J.-M. MOREL

Partial Differential equations and image smoothing

Vicent Caselles, Bartomeu Coll and Jean-Michel Morel

July 12, 1996

Abstract

We try to answer the following question, crucial in digital image processing : Is image smoothing possible ? We give an essentially negative answer based on the physics of image generation and consequent invariance requirements which we prove not to be possibly matched by any local smoothing operation. We temper this negative result by showing that local image smoothing is possible provided singular points of the image have been previously detected and preserved. We define the associated degenerate partial differential equation and sketch the proof of its mathematical validity. Our analysis uses the phenomenological theory of image perception of Gaetano Kanisza, whose mathematical translation yields an algorithm for the detection of the discontinuity points of digital images.

1   Introduction

Images, in a continuous model, are functions $u(x)$ defined on a domain Ω of the plane, generally a rectangle. Let us consider, without much loss of generality, grey level images, that is is, images where $u(x)$ is a real number between (say) 0 and 255 denoting the "grey level" or brightness. In practice, images are *digitized*, which means that values of $u(x)$ are given only in a discrete grid of a rectangle. It is, however, very convenient to discuss the geometry of images in the continuous framework of functional analysis. This passage to a continuous model is valid provided if it is shown that algorithms defined in the continuous model can be made effective on their digitized trace.

We shall in this conference sketch the process of image formation and deduce which kind of geometric structure images are then expected to have. We shall be particularly interested in the singularities of the image which are inherent to the formation process. We shall then discuss whether smoothing procedures which have been proposed in the past in order to smooth the image (and thereafter compute derivatives of the smoothed image) are compatible or not with the image formation process. In short : can a smoothing process be performed, which does not destroy what it ought to detect, the image structure ? We shall see that the answer is close to negative, and show that in fact *singularities in the image must be detected previously to any smoothing procedure*. An image smoothing operator, in a very restrictive way, can then be defined and we shall explain how.

It would be very useful to compute derivatives of any order on an image $u(x)$. The datum being at first sight discontinuous everywhere, this looks desesperate if some notion of scale is not introduced. The scale parameter, which we denote by t, measures the degree of smoothing we allow in an image. Scale $t = 0$ corresponds to the actual image, and we denote by $u(t, x)$ the image smoothed at scale t. Let us, without criticism for the first review, list the smoothing processes proposed so far. In all of these processes, described by parabolic P.D.E.'s, we set $u(0, x) = u(x)$, the initial datum. In the forthcoming formulas, $\Delta u = \frac{\partial^2 u}{\partial x^2} + \frac{\partial^2 u}{\partial y^2}$ denotes the Laplacian of $u(t, x, y)$ with respect to the space variables (x, y), $Du = (\frac{\partial u}{\partial x}, \frac{\partial u}{\partial x})$ its spatial gradient and $curv(u) = div(\frac{Du}{|Du|})$ the curvature of the level line, where $|Du|$ is the euclidean norm of Du and $div = \frac{\partial}{\partial x} + \frac{\partial}{\partial y}$. The main smoothing equations we have in mind are

- The heat equation [Wi] :

$$\frac{\partial u}{\partial t} = \Delta u$$

- The mean curvature motion (Osher-Sethian equation [OS])

$$\frac{\partial u}{\partial t} = |Du|curv(u)$$

- The A.M.S.S. model ([AGLM1], [ST1])

$$\frac{\partial u}{\partial t} = |Du|curv(u)^{\frac{1}{3}}.$$

Other diffusion equations have been proposed for image smoothing, but the ones listed here have more invariance or conservation properties and are enough to launch

the discussion. It is proven that the heat equation is the only linear, isotropic image smoothing model, and the A.M.S.S. model is the only contrast invariant, affine invariant image smoothing model. The Osher-Sethian equation is somehow an intermediate case, being both quasilinear and constrast invariant.

The heat equation performs beautifully as for the initial mentionned aim, the computation of derivatives of any order in an image. Now, it is not contrast invariant. Constrast invariance means that the smoothing operator $T_t : u \rightarrow u(t) = T_t u$ commutes with contrast changes g. Any nondecreasing real function g is an admissible contrast change and the observed values $u(x)$ are in practice defined up to an unknown contrast change. The third considered model has been proposed as the most invariant smoothing model in [AGLM1], [ST1]. We refer to [AM1] for a very synthetical proof of its uniqueness. There is, however, a significant objection to the second and third models : in order to make sense mathematically, they request that the initial image be continuous ! We shall see in the next section that this is a not a realistic requirement for images. If we remove this requirement, we can still draw the same conclusions as in [AGLM], but only locally, at points where the image is not discontinuous, which we call singular points. This will become clear from the discussion below.

Our plan is as follows. In Section 2, we show how the image formation process entails generation of singularities and leads to invariance requirements for the image operators. In Section 3, we deduce which are the largest invariant objects (or "atoms") in an image which can be taken as initial data for smoothing operations : we prove that they consist in pieces of level lines of the image joining singular points. Section 4 is devoted to the effective computation of "atoms" and singular points of the image and to first experiments. In Section 5 we finally join our aim, which is to propose a P.D.E. model with the right boundary conditions at image singular points. We prove experimentally that the visual aspect of images is not altered by such a structure preserving smoothing process. An experiment shows how, thanks to the smoothing thus defined, we can transform an image into a topographic map revealing the structure of the image and its essential singularities. This conference text presents some of the arguments, experiments and proofs which are extensively developed in an article to appear ([CCM]). The axiomatic theory of image smoothing which we use is the object of a book to appear ([GM]).

2 How images are generated : occlusion and transparency as basic operations

In this section, we make two concrete assumptions about the kind of image in consideration. We first assume that those images are obtained by a photographic device, that is, a camera sensible to visible spectrum. We restrain the study to the case of grey level images. Second, we assume that the photographs thus taken come from a natural, human or animal, environment and therefore roughly correspond to common retinian images. This may seem a very vague assertion, but we shall give it a precise sense in the following.

2.1 Occlusion as a basic operation on images

Natural, human visual world is made of objects of many sizes and heights which are spread out on the ground. Since the observer or the camera are assumed to be put close to the ground level, it is assumed that those objects tend to occlude each other. As pointed out by the phenomenologist Kanizsa [Ka], we generally see only parts of the objects in front of us because they occlude each other. Let us formalize this by assuming that objects have been added one by one to a scene. Given an object $\tilde{A}$ in front of the camera, we call A the region of the image onto which it is projected by the camera. We call u_A the part of the image thus generated, which is defined in A. Assuming now that the object $\tilde{A}$ is added in a real scene $\tilde{R}$ of the world whose image was v, we observe a new image which depends upon which part of $\tilde{A}$ is in front of objects of $\tilde{R}$, and which part in back. Assuming that $\tilde{A}$ occludes objects of $\tilde{R}$ and is occluded by no object of $\tilde{R}$, we get a new image $u_{\tilde{R}\cup\tilde{A}}$ defined by

$$u_{\tilde{R}\cup\tilde{A}} = u_A \text{ in } A \text{ and}$$
$$u_{\tilde{R}\cup\tilde{A}} = v \text{ in } I\!\!R^2 \setminus A. \quad (1)$$

Of course, we do not take into account in this basic model the fact that objects in $\tilde{R}$ may intercept light falling on $\tilde{A}$, and conversely. In other terms, we have omitted the shadowing effects, which will now be considered.
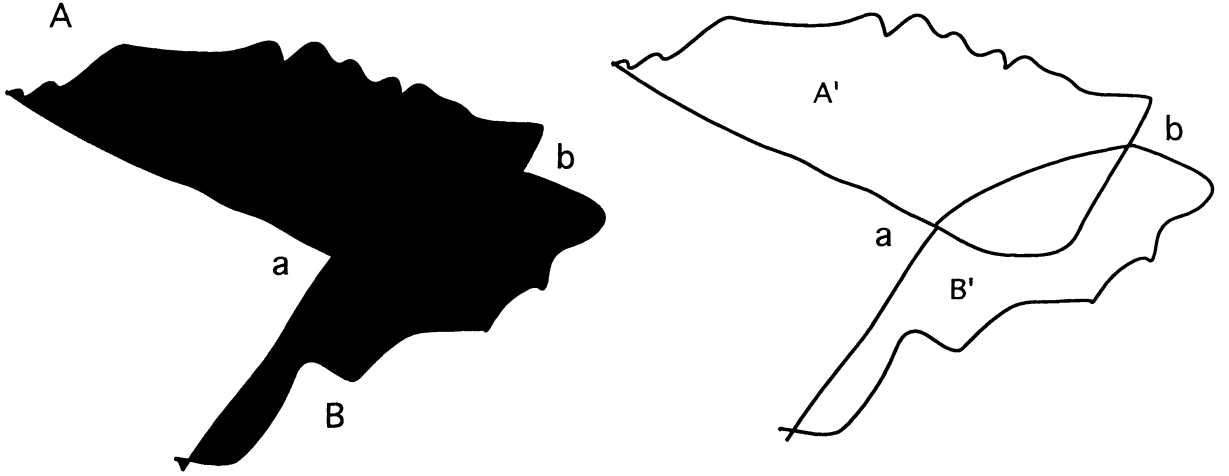
Figure B. T-junctions and occlusions : the lefthand figure, composed of two regions A and B is interpreted as the superposition of two objects A' and B' which are represented on the right by their contours. The completion thus effectuated by a low level vision process consists in extending beyond the T-junctions a and b the boundary of the object B', which apparently "stops" when it meets the object A'. This interruption is interpreted as an occlusion.

2.2 Transparency (or shadowing) as a second basic operation on images

Let us assume that the light source is a point in euclidean space, and that an object $\tilde{A}$ is interposed between a scene $\tilde{R}$ whose image is v and the light source. We call $\tilde{S}$ the shadow spot of $\tilde{A}$ and S the region it occupies in the image plane. The resulting image u is defined by

$$u_{\tilde{R},\tilde{S},g} = v \text{ in } I\!R^2 \setminus S \text{ and}$$
$$u_{\tilde{R},\tilde{S},g} = g(v) \text{ in } S. \qquad (2)$$

Here, g denotes a contrast change function due to the shadowing, which is assumed to be uniform in $\tilde{S}$. Clearly, we must have $g(s) \leq s$, because the brightness decreases inside a shadow, but we do not know in general how g looks. The only assumption for introducing g is that points with equal grey level s before shadowing get a new,

but the same, grey level $g(s)$ after shadowing. Of course, this model is not true on the boundary of the shadow, which can be blurry because of diffraction effects or because the light source is not really reducible to a point. Another problem is that g in fact depends upon the kind of physical surface which is shadowed so that it may well be different on each one of the shadowed objects. This is no real restriction, since this only means that the shadow spot S must be divided into as many regions as shadowed objects in the scene ; we only need to iterate the application of the preceding model accordingly. A variant of the shadowing effect which has been discussed in perception psychology is *transparency*. In the transparency phenomenon, a transparent homogeneous object $\tilde{S}$ (in glass for instance) is interposed between part of the scene and the observer. Since $\tilde{S}$ intercepts part of the light sent by the scene, we still get a relation like (2), so that transparency and shadowing simply are equivalent from the image processing viewpoint. If transparency (or shadowing) occurs uniformly on the whole scene, Relations (2) reduces to

$$u_g = g(v),$$

which means that the grey-level scale of the image is altered by a nondecreasing contrast change function g.

2.3 Requirements for image analysis operators

Of course, we do not know *a priori*, when we look at an image, what are the physical objects which have left a visual trace in it. We know, however, that the operations having led to the actual image are given by formulas (1)-(2). Thus, any processing of the image should avoid to destroy the image structure resulting from (1)-(2) : this structure traduces the information about shadows, facets and occlusions which are clues to the physical organization of the scene in space. *The identity and shape of objects must be recovered from the image by means which should be stable with respect to these operations.* As a basic and important example, let us recall how the Mathematical Morphology school has insisted on the fact that image analysis operations must be invariant with respect to any contrast change g. In the following, we shall say that an operation T on an image u is *morphological* if

$$T(g(u)) = T(u)$$

for any nondecreasing contrast change g.

3 Consequences of image formation : basic objects of image analysis

We call *basic objects* a class of mathematical objects, simpler to handle than the whole image, but into which any image can be decomposed and from which it can be reconstructed. The classical examples of image decompositions are

• Additive decompositions into simple waves : Basic objects of Fourier analysis are cosine and sine functions, basic objects of Wavelet analysis are wavelets or wavelet packets, basic objects of Gabor analysis are windowed (gaussian modulated) sines and cosines. In all of these cases the decomposition is an additive one, not adapted to the structure of images, except perhaps for restoration processes in presence of additive noise. Indeed, operations leading to the construction of real world images are strongly nonlinear and the simplest of them, the constrast change, does not preserve additive decompositions. If $u = u_1 + u_2$, then it is not true that $g(u) = g(u_1) + g(u_2)$ if the constrast change g is nonlinear.

• Next, we have the representation of the image by a *segmentation*, that is, a decomposition of the image into homogeneous regions separated by boundaries, or "edges". The criterion for the creation of edges or boundaries is the strength of constrast on the edges, along with the homogeneity of regions. Both of these criteria are simply not invariant with respect to contrast changes. Indeed $\nabla g(u) = g'(u)\nabla u$ so that we can alter the value of the gradient by simply changing the constrast.

• Finally, we can decompose, as proposed by the Mathematical Morphology school, an image into its binary images (or level sets) obtained by thresholding. We set $X_\lambda u(x) = white$ if $u(x) \geq \lambda$ and $X_\lambda u(x) = black$ otherwise. The white set is then called *level set* of u. It is easily seen that, under fairly general conditions, an image can be reconstructed from its level sets by the formula

$$u(x) = \sup\{\lambda, u(x) \geq \lambda\} = \sup\{\lambda, x \in X_\lambda u\}.$$

The decomposition therefore is nonlinear, and reduces the image to a family of plane sets (X_λ). In addition, if we assume that the level sets are Cacciopoli subsets of $I\!\!R^2$, that is sets whose boundary has finite length, then a classical theorem asserts that its boundary is a union of closed Jordan curves (see [MS], Chapter 6). In the discrete framework, this theorem is obvious and we can associate with each level set

a finite set of Jordan curves which define its boundary. Conversely, the level set is uniquely defined from those Jordan curves. We shall call them *level curves of the image*. Are level sets and level curves the sought for basic objects of image processing? In some sense they are better than all above discussed "basic objects" because they are invariant under contrast changes. To be more precise, if we transform an image u into gou, where g is an increasing continuous function (understood as a contrast change), then it is easily seen that the set of level sets of gou is equal to the set of level sets of u.

However, level sets are drastically altered by occlusion or shadowing. Let us discuss this point. One can see in Figure 4 an elementary example of image generated by occlusion. A grey disk is partly occluded by a darker square (a). In (b) we display a perspective view of the image graph. In (c) and (d) we see two of the four distinct level sets of the image, the other ones being the empty set and the whole plane. It is easily seen that none of the level sets (c) and (d) corresponds to physical objects in the image. Indeed, one of them results from their union and the other one from their set difference. The same thing is true for the level lines (e) and (f) : they appear as the result of some "cut and paste" process applied to the level lines of the original objects. It is nontheless true, because of the invariance with respect to constrast changes, that the basic objects of image processing must be somehow parts of the level lines. This leads us to what will be our proposition.

• *Our proposition : Basic objects are all junctions of level lines, (particularly : T-junctions, τ-junctions, X-junctions, Y-junctions) and parts of level lines joining them.*
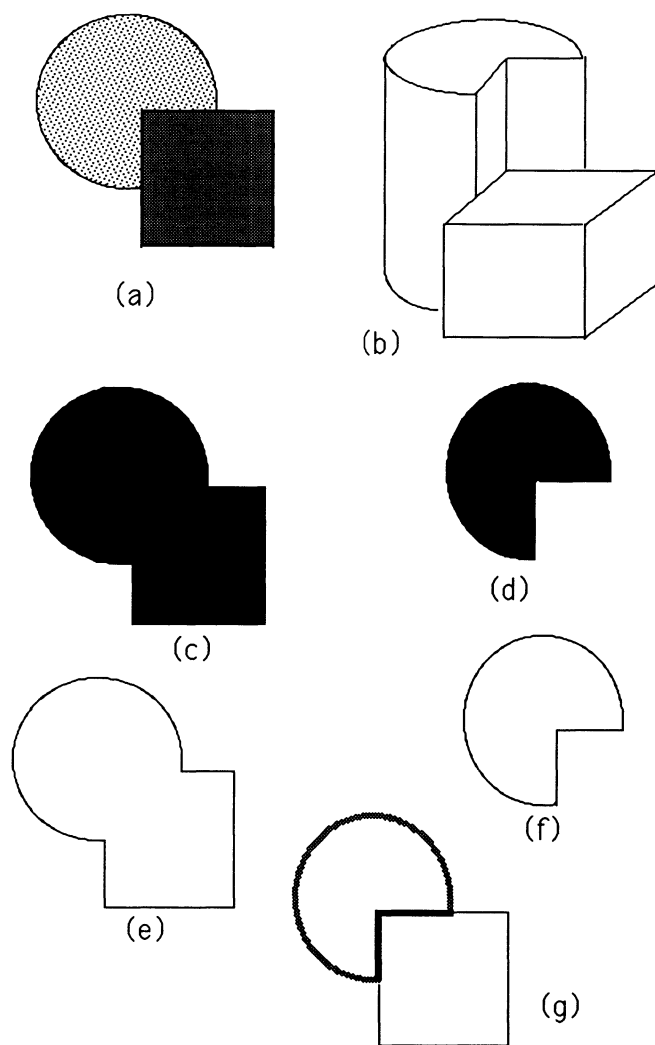
figure 4 : Image, level sets, level lines
and T-junctions.

The terms contained in this proposition will be explicited one by one, starting with T-junctions. We again refer to Figure 4 for a first simple (but, in fact, general) example. The level lines (e) and (f) represent two level lines at two different levels and in (g) we have superposed them in order to put in evidence how they are

organized with respect to each other. We have displayed one of them as a thin line, the other one as a bold line and the common part in grey. The T-junctions can be defined in such an ideal case as the points where two level lines corresponding to two different levels meet and remain together. Let us start with some simple phenomenology of junctions.
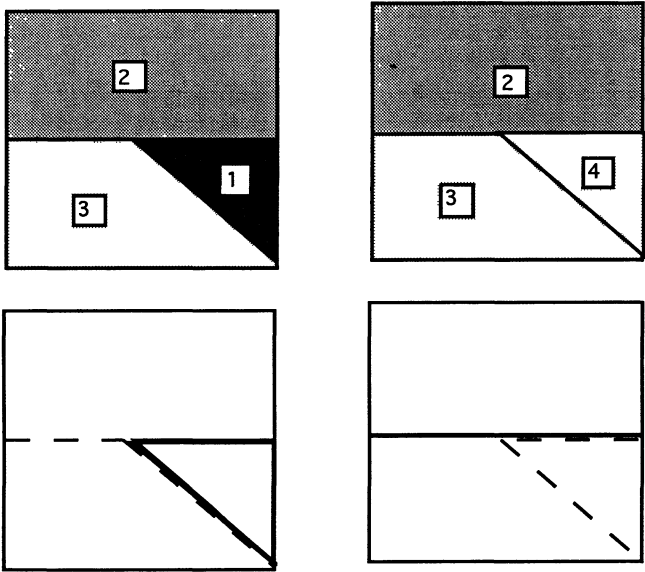

Figure 5 : The two kinds of T-junctions
depending on the ordering of grey levels

3.1   T-junctions

As shown in Figure 5, there are two possibilities which depend upon the order of grey levels around the T-junction. In the first case, the T-junction appears as two joint level lines taking at the junction two opposite directions. In the second case, one of the level lines is locally straight and the other one has two branches, one of which coincides with the first level line. Thus a T-junction at a point x can be (a little bit naively) described in the following way.

- Two level lines meet at point x.

- The half level lines (or branches) starting from x are thus four in number ; two

coincide and two take opposite directions. (The branches which coincide belong to different level lines. The branches which take opposite directions may also belong to the same level line or not).

3.2 Transparencies and X-junctions

The next case of singularity is caused by the transparency phenomenon and we shall call it X-junctions. In the transparency phenomenon, we have assumed that inside a spot S, an original image v is changed into $u = g(v)$, where g is a contrast change. We keep $u = v$ outside the spot S. As a consequence, a level line with level λ outside S becomes a level line with level $g(\lambda)$ inside the spot, so that the level lines inside S are continuations of level lines outside S. Fuchs showed that this results in the *continuation* perceptual phenomenon : we tend to see the visible edges of v crossing the boundary of S [F]. Of course, this illusion is based on the continuity of direction. In the same way, of course, the boundary of S is seen as crossing the level lines of v. In fact, level lines cannot cross and the behaviour of level lines is analyzed in Figure 9. In the transparency phenomenon, the apparent crossing, which we shall call X-junction, consists in the meeting at a point x of two level lines. These level lines locally create four angular regions. Without loss of generality, we can assume that the angular regions have grey levels 1, 2, 3 and 4. Indeed, the grey levels need not be constant inside each region, but we know that the ranges of the four angular regions are ordered. This is an obvious consequence of the fact that each pair of regions is separated by a level line. Then we see that three cases may occur, which are shown in Figure 9.
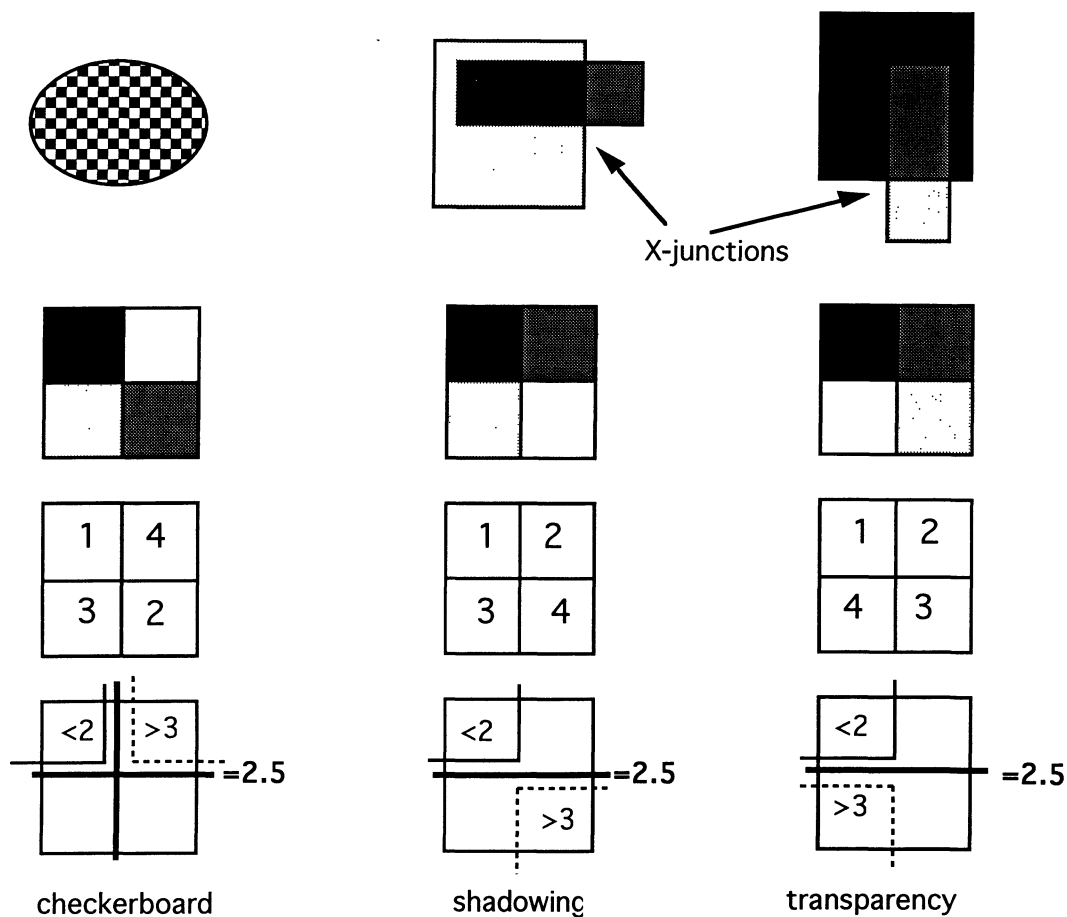
Figure 9. The three kinds of X-junctions. We first display (above) three kinds of visual experiments which lead respectively to checkerboard, shadowing and transparency sensations. The second and third rows focus on the resulting X-junctions and the local grey level values. The last row shows the resulting configuration of level lines. By "=2.5", we denote the level lines separating the regions 1 and 2 from 3 and 4.

• First case : "checkerboard". The higher grey levels 3 and 4 are in two diagonally opposite regions and the lower grey levels 1 and 2 in the other two opposite regions. (The perfect checkerboard case corresponds to 3=4 and 1=2, but we display a more general case with the same structure for level lines). The checkerboard

singularity does not seem to correspond to many physical phenomena, but is non-theless frequent in the human world, probably for the designer's pleasure of showing a parodoxal, physically impossible, visual situation. In this case, we can see how an intermediate level line forms a cross.

• Second case : "shadowing". The lower regions 1 and 2 are adjacent and so are the regions 3 and 4. In addition, 1 is adjacent to 3 and 2 to 4. Somehow, this situation is the most stable and least paradoxical of all, since it can be interpreted as the crossing of a shadow line with an edge. It is worth noticing that in this case the level line which separates the sets $\{x, u(x) > 2\}$ and $\{x, u(x) < 3\}$ can be interpreted indifferently as the shadow line or the edge line. The other (shadow or edge) line has no existence as a level line, but is obtained by concatenating two branches of two distinct level lines. The level lines bounding the sets $u > 1$ and $u > 3$ only meet at point x and form the "X-junction" which we shall trace in experiments on real images.

• Third case : "transparency". The regions 1 and 2 with lower grey-level and the higher grey-level regions 3 and 4 are again adjacent, but the pairs of extreme regions also are adjacent : 1 to 4 and 2 to 3. The transparent material is adding its own color, which is assumed here to be light grey, so that white becomes light grey and black becomes dark grey. The interpretation is not twofold in this case : the original edge (horizontal in the figure) must be the level line bounding the set $u > 2$. The shadow line (vertical in the figure), is built with two branches of distinct level lines.

3.3   Discussion of the decomposition into basic objects

Let us summarize our proposition for basic objects, or "atoms" of image processing. It consists in arguing about the invariance of the image analysis with respect to the accidents of the image generation.

Argument 1 *(Invariance Argument)*

• *Since the image formation may include an unknown and non recoverable contrast change : We reduce the image to its parts invariant with respect to contrast changes, that is, the level lines.*

• *Since, every time we observe two level lines (or more) joining at a point, this can be the result of an occlusion or of a shadowing, we must break the level lines at this point : indeed, the branches of level lines arriving at a junction are likely to be parts of different visual objects (real objects or shadows). As a consequence, every junction is a possible cue to occlusion or shadowing.*

A remarkable point about Argument 1 is that it needs absolutely no assumption about the physical objects, but only on the "final" part of image generation by contrast changes, occlusions and shadowing. The conclusion of Argument 1 coincides with what is stated by phenomenology [Ka, 1, 2]. Indeed, Gaetano Kanizsa proved the main structuring role of T and X-junctions in our interpretation of images. Of course, he does not give indications on how these junctions should be detected, but Argument 1 shows that there is a canonical way to do the detection.

4 Computation of basic objects in a digital image

4.1 Algorithm computing basic objects

In this section, we discuss how the atoms discussed above can be detected in digital images and we present experimental results. The above description of T- and X-junctions is based on the assumptions that

• Level sets and level lines can be computed.

• The meeting of two level lines with different levels can be detected.

In a digital image, the level sets are computed by simple thresholding. A level set $\{u(x) \geq \lambda\}$ can be immediately displayed in white on black background. In the actual technology, $\lambda = 0, 1, ..., 255$, so that we can associate with an image 255 level sets. The Jordan curves limiting the level sets are easily computed by a straightforward algorithm : they are chains of vertical and horizontal segments limiting the pixels. In the numerical experiments, these chains are represented as chains of pixels by simply inserting" boundary pixels" between the actual image pixels. In order to get a correct visual representation of level lines, we therefore apply a zoom with

factor 2.

We define "junctions" in general as every point of the image plane where two level lines (with different levels) meet. The meeting of two level lines can be considered as physically meaningful if and only if the level lines diverge significantly from each other. In order to distinguish between the true junctions and the ones due to quantization effects, we decide to take into account T-junctions if and only if

- the area of the occulting object is large enough,
- the apparent area of the occulted object is large enough and
- the area of background is large enough too.

This threshold on area must be of course as low as possible, because there is a risk to loose T-junctions between small objects. Small size significant objects appear very often in natural images : they may simply be objects seen at a large distance. In any case, the area threshold only depends on the quantization parameters of the digital image and tends ideally to zero when the accuracy of the image tends to infinite. The algorithm for the elimination of dubious junctions is as follows.


Junction Detection Algorithm

- Fix an area threshold n (in practice, $n = 40$ pixels seems sufficient to eliminate junctions due to quantization effects.)

- Fix a grey level threshold b (in practice : $b = 2$ is sufficient to avoid grey level quantization effects).

- At every point x where two level lines meet : define $\lambda_0 < \mu_0$ the minimum and maximum value of u in the four neighboring pixels of x.

- We denote by L_λ the connected component of x in the set $\{y, u(y) \leq \lambda\}$ and by M_μ the connected component of x in the set $\{y, u(y) \geq \mu\}$. Find the smallest $\lambda \geq \lambda_0$ such that the area of L_λ is larger than n. Call this value λ_1. Find the largest $\mu, \lambda_1 \leq \mu \leq \mu_0$, such that the area of M_μ is larger than n. We call this value μ_1.

- If λ_1 and μ_1 have been found, if $\mu_1 - \lambda_1 \geq 2b$, and if the set $\{y, \mu_1 - b \geq u(y) \geq \lambda_1 + b\}$ has a connected component containing x with area larger than n, then retain x as a valid junction.
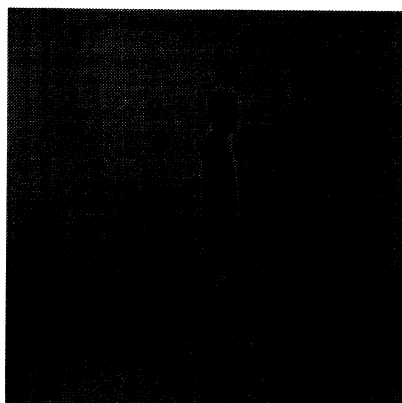
4.2 Experiments

The experiments have been made on WorkStation SUN IPC, with the image processing environment MegaWave II, whose author is Jacques Froment.

● **Experiment 1 : The boolean structure of occlusion retrieved by level set analysis in two successive images of a sequence.** The eight images $u_1, ..., u_8$ of the experiment are displayed from left to right and from top to bottom. The images u_1 and u_2 are grey-level images and the other ones are binary images (black and white) which display level sets and logical operations effectuated on them. The coding convention is $black = 0 = false$, $white = 255 = true$, so that we identify level sets with binary images and union with max, intersection with min and set difference with ” $-$ ”. We first see *el caminante* (a walking researcher, photographed by Paco Perales) in two successive positions u_1 and u_2. Then *el caminante* without skirting-board : $u_3 = \{x, u_1(x) > 10\}$ and *el caminante* with skirting-board $u_4 = \{x, u_1(x) > 70\}$. Next, $u_5 = u_4 - u_3$, that is, the skirting-board without the walking man, $u_6 = \{x, u_2(x) > 70\}$, *El caminante* with skirting-board in Position 2. Finally $u_7 = max(u_3, u_6)$: the resulting black parts display the part of the skirting-board occluded in Position 1 plus the part of the ground which remains occluded by the feet of the *caminante* in both images. In $u_8 = min(u_7, u_5)$, we display the reconstruction of the whole skirting-board by adding the occluded part in Position 1 deduced from Position 2.

● **Experiment 2 : detection of T-junctions as meeting points of level lines.** The original grey-level image is u_1. In u_2 we see *El caminante* with skirting-board : $u_1 > 60$ and u_3 is *El caminante* without skirting-board. We display in u_4 the level lines of u_2 in white and the level lines of u_3 in black with their common parts in dark grey. Candidates to T-junctions generated by the main occlusions can be seen. They are characterized as meeting points of a black, a white and a grey line. In u_5, we see all T-junctions detected from those two level sets, after a filtering of spurious T-junctions has been made, with area threshold $n = 80$.
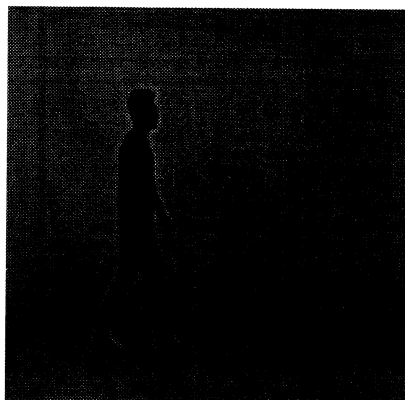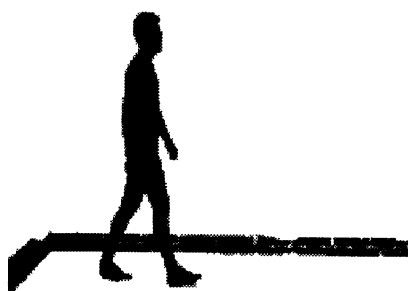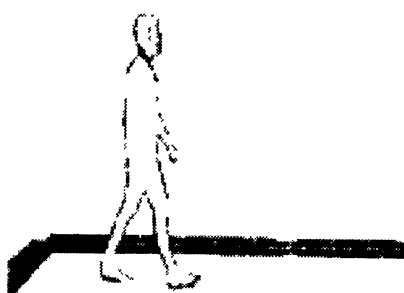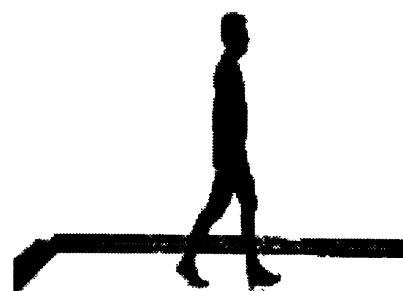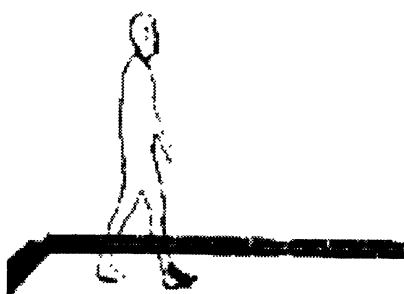
u1
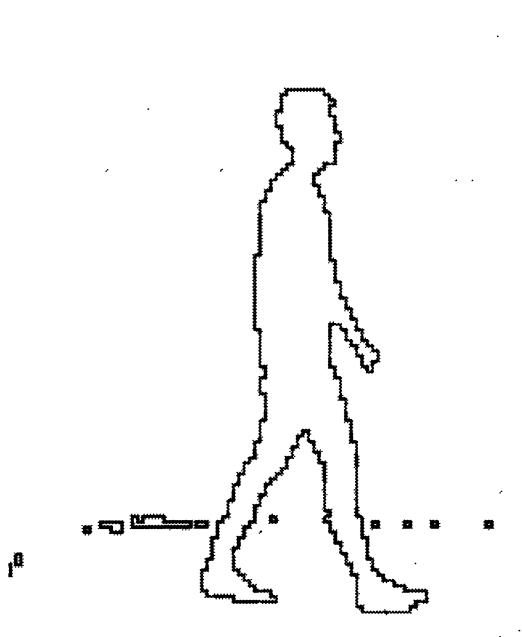
u2

u3

u4

u5

u6

u7

u8

Experiment 1.

u1

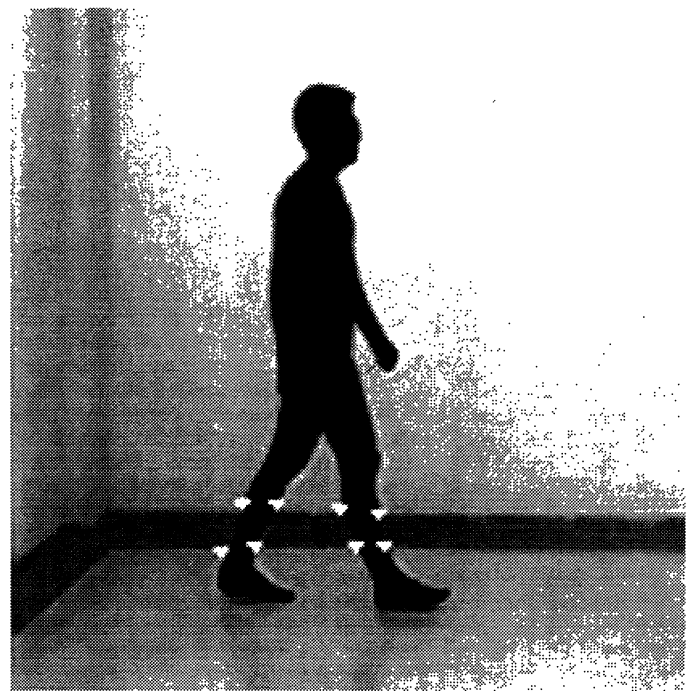

u2

u3

u4

u5

Experiment 2.

5 Image filtering preserving Kanizsa singularities

5.1 Image and level curve smoothing models

In this section, we push a little further the exploration of invariant image or level lines filtering methods which have been recently proposed in [AGLM1] and [ST1]. According to the axiomatic presentation of image iterative smoothing (or "pyramidal filtering", or "scale space") proposed in [AGLM1], all iterative filtering methods, depending on a scale parameter t, can be modelized by a diffusive partial differential equation of the kind

$$\frac{\partial u}{\partial t}(t, x, y) = F(D^2u(t, x, y), Du(t, x, y), x, y, t), \quad u(0, x, y) = u_0(x, y),$$

where $u_0(x, y)$ is the initial image, $u(t, x, y)$ is the image filtered at scale t and Du, D^2u denote the first and second derivatives with respect to (x, y). (We set $Du(x, y) = (\frac{\partial u}{\partial x}(x, y), \frac{\partial u}{\partial y}(x, y)) = (u_x, u_y)(x, y)$ and in the same way, we define $D^2u(x, y)$ as the symmetric matrix of second partial derivatives $u_{xx}, u_{xy}, u_{yx}, u_{yy}$ of u with respect to x and y.)

The most invariant "scale space" proposed in [AGLM1], is the Affine Morphological Scale Space, that is, an equation of the preceding kind which is invariant with respect to contrast changes of the image and affine transforms of the image plane,

$$(AMSS) \quad \frac{\partial u}{\partial t} = |Du|(curv(u))^{\frac{1}{3}}, \quad u(0, x, y) = u_0(x, y),$$

where

$$curv(u)(x, y) = \frac{u_{xx}(u_y)^2 - 2u_{xy}u_xu_y + u_{yy}(u_x)^2}{(u_x^2 + u_y^2)^{\frac{3}{2}}}(x, y)$$

is the curvature of the level line passing by (x, y). The interpretation of the AMSS model is given in [AGLM1] and corresponds to the following evolution equation for curves, proposed independently in [ST1] and which we call (ASS) (Affine Scale Space of curves)

$$(ASS) \quad \frac{\partial C}{\partial t}(t, s) = (curv(C(t, s)))^{\frac{1}{3}}\vec{n}(t, s), \quad C(0, s) = C_0(s),$$

where $C(0, s)$ is an initial curve embedded in the plane and parameterized by s, $\vec{n}(t, s)$ is the normal unit vector at $C(t, s)$ and $curv(C(t, s))$ the curvature of the

curve at $C(t, s)$. The relation between (AMSS) and (ASS) is formally the following :
(AMSS) moves all level lines of $u(t, x, y)$ as if each one were moving by (ASS). At
the mathematical level, however, existence and uniqueness results are not at the
same stage. (AMSS) has been proved to have a unique solution in the viscosity sense
when the initial image is continuous. (ASS) is proved so far to have a unique smooth
solution when the initial curve is convex. *The main drawback of the classification
proposed in [AGLM1] is the (necessary) assumption that the initial image $u_0(x)$ is
continuous with respect to x.* Without this assumption, the (AMSS) model and the
related morphological models loose mathematical consistency. This drawback can
be avoided by using the Osher-Sethian [OS] method : If we wish to apply (AMSS)
to (e.g.) a binary and therefore discontinuous image $\mathbb{1}_X$, we substitute to $\mathbb{1}_X$ the
signed distance function u_0 to X, which is Lipschitz and has X as zero level set :
$X = \{x, u_0(x) \leq 0\}$. We apply to u_0 the (AMSS) model and define the evolution
of X as the zero level set of $u(t)$. Evans and Spruck [ES] have shown that such
an evolution does not depend upon the chosen distance function and coincides with
(ASS) when the evolution of the boundary of X is well defined and smooth. In other
terms, we can use (AMSS) either for moving continuous functions, or for moving a
single set, or a single Jordan curve, by moving its distance function. In order to deal
with general discontinuous functions, we deduce that the (AMSS) evolution will be
well defined only if we can reduce it to the joint motion of single level curves.

5.2 A Kanizsa model for image evolution

Here, we refer to our discussion on the basic objects of Image Analysis, in Section
3. According to this discussion, the decomposition of u_0 into its level lines followed
by a further independent analysis of each is not correct : indeed, level lines interact
at all image singularities (T-, X-junctions,...) and we have argued that atoms of
the image must be the pieces of level lines joining junctions and not the level lines
themselves. In other terms, a correct atomic decomposition of the image implies a
previous *segmentation* of the level lines. After this segmentation only, the smoothing
described by (AMSS) or (ASS) can be applied. This means that we are allowed
to move the level lines (for smoothing, or multiscale analysis purposes) but with
internal boundary conditions : the level lines being during their motion constrained
to pass by their endpoints, the junctions. The image model which arises from the
preceding discussion is following.

Definition 1 *(Kanizsa image model)*
We call image a function $u(x)$ whose level lines have all a finite length and meet only on a closed set without interior $\mathcal{Z}$, which we call the set of junctions of u.

When the junction set is finite (which is the case for digital images), we set $\mathcal{Z} = \{z_1, z_2, ..., z_n\}$. According to the preceding discussion, the correct adaptation of the (AMSS) model to images having junctions is

Algorithm 1 : Junctions-preserving, affine invariant and contrast invariant smoothing
• Compute the junctions $z_1, z_2, ..., z_n$ (by the Junction Detection algorithm, which is affine invariant).

• Move each piece of level curve C by the (ASS) model. If the curve has endpoints, they remain fixed and the (ASS) evolution is not allowed to let the curve cross other junctions. This yields $C(t)$.

• Reconstruct a smoothed image $u(t, x, y)$ which has the curves $C(t)$ as level lines and the z_i as junctions. This reconstruction is possible because the (ASS) model preserves the inclusion of curves (see [AM])

Let us give a variant of the preceding algorithm which permits a progressive removal of junctions (according to their scale).

Algorithm 2 : progressive removal of junctions
For every t, starting from $t = 0$:
• Compute the junctions $z_1, z_2, ..., z_n$ (by an affine invariant algorithm).

• Move each piece of level curve C by the (ASS) model, as specified in Algorithm 1. This yields $C(t)$.

• Remove at scale t all junctions which do not meet anymore the requirements of the Junction Detection Algorithm with respect to the new level curves $C(t)$.

• Reconstruct a smoothed image $u(t, x, y)$ which has the curves $C(t)$ as level lines and the remaining z_i as junctions.

In the next subsubsection, we shall discuss how to implement Algorithm 1, Algorithm 2 being a variant including in its loop the Junction Detection Algorithm.

5.2.1 Mathematical and numerical discussion of Algorithms 1, 2

Both algorithms (1 and 2) are well defined provided the (ASS) model is mathematically correctly posed ; this point is, however, still not completely solved. In addition, the independent processing of all pieces of level lines looks computationally heavy. So we prefer to consider a variant of (AMSS) implementing Algorithms 1 and 2. We consider the characteristic function $\mathbb{1}_{\mathcal{Z}}(x,y) = 0$ if $(x,y) \in \mathcal{Z}$ and $\mathbb{1}_{\mathcal{Z}}(x,y) = 1$ if $(x,y) \notin \mathcal{Z}$ of the junctions and apply to the original image the equation

$$(AMSS1) \qquad \frac{\partial u}{\partial t} = \mathbb{1}_{\mathcal{Z}}(x,y)|Du|(curv(u))^{\frac{1}{3}}, \quad u(0,x) = u_0(x).$$

We conjecture that such an equation makes sense, and has a unique viscosity solution (in the sense defined in [CIL]) preserving the singularities and moving each piece of level line by the (ASS) model. In addition, we conjecture that the pieces of level lines joining junctions keep the same endpoints by such a process. We shall discuss in the next section in which way well-posedness can be proved for (AMSS1).

Let us now consider a well-posed approximation of (AMSS1). We replace $\mathbb{1}_{\mathcal{Z}}$ by a function $\mathbb{1}_{\mathcal{Z},\varepsilon}$ which is smooth (e.g. C^∞) and satisfies

$$\mathbb{1}_{\mathcal{Z},\varepsilon}(x,y) = 1$$

if the distance of (x,y) to $\mathcal{Z}$ is larger than ε and

$$\mathbb{1}_{\mathcal{Z},\varepsilon}(x,y) = 0$$

if the distance of (x,y) to $\mathcal{Z}$ is smaller than $\frac{\varepsilon}{2}$ and $0 \le \mathbb{1}_{\mathcal{Z},\varepsilon} \le 1$ everywhere. This function simply is a smooth approximation of the characteristic function of Z, $\mathbb{1}_{\mathcal{Z}}$, for which we can directly apply known existence and uniqueness theorems. The considered model therefore is

$$(AMSS_\varepsilon) \qquad \frac{\partial u}{\partial t} = \mathbb{1}_{\mathcal{Z},\varepsilon}(x,y)|Du|(curv(u))^{\frac{1}{3}}.$$

and it is an equation of the kind

$$\frac{\partial u}{\partial t}(t,x,y) = F(D^2u(t,x,y), Du(t,x,y), x, y), \quad u(0,x,y) = u_0(x,y),$$

where F is continuous with respect to all variables, nondecreasing with respect to its first argument and satisfying the condition

$$(3) \quad \forall x \in I\!\!R^2, \quad F(0,0,x) = 0,$$

and some additional continuity conditions for F which are easily checked in our case. Then, as it is proved in [GGIS], $(AMSS_\varepsilon)$ has a unique solution in the viscosity sense. Therefore, it also satisfies a local comparison principle. Indeed, by Theorem 4.2 in [GGIS], we have a comparison principle between sub- and supersolutions of $(AMSS_\varepsilon)$. Moreover, because of (3), constant functions are solutions of $(AMSS_\varepsilon)$, and, as in [CGG] Theorem 4.5, by using [CGG] Proposition 2.3 and the comparison principle mentioned before, one can construct by the Perron method a (unique) viscosity solution for $(AMSS_\varepsilon)$. In this argument, we have assumed that the image is defined in all of $I\!\!R^2$. This does not matter, since we can impose without loss of consistency in our model that all points on the boundary of our image are T-junctions. Then the image can be extended by 0 to the whole plane. Another point to make clear in the application of the above theorems is following : the existence and uniqueness results apply only if the initial datum u_0 is continuous, which is not our case. So we can argue in the following way. Let us call $\mathcal{Z}_\varepsilon$ the ε-neighborhood of $\mathcal{Z}$. We know that outside $\mathcal{Z}_{\frac{\varepsilon}{2}}$ the function u_0 is continuous. We can, by Tietze Theorem, extend u_0 inside $\mathcal{Z}_{\frac{\varepsilon}{2}}$ as a continuous function, which we call $\tilde{u}_0$. Then the existence and uniqueness theorems mentioned above apply. It only remains to prove that the solution thus obtained does not depend upon the choice of the extension $\tilde{u}_0$. Indeed, it is easily seen that inside $\mathcal{Z}_{\frac{\varepsilon}{2}}$ solutions of $(AMSS_\varepsilon)$ with continuous initial data does not move. We deduce, as an easy consequence of the comparison principle, that all continuous extensions of u_0 inside $\mathcal{Z}_{\frac{\varepsilon}{2}}$ yield the same solution outside.

The interpretation of $(AMSS_\varepsilon)$ is essentially the same as for $(AMSS1)$: the level lines of u with endpoints on $\mathcal{Z}$ are constrained to keep the same endpoints and the only difference with respect to $AMSS1$ is an alteration of their speed in an ε-neighborhood of $\mathcal{Z}$. Of course, it is more than likely that the solution of $(AMSS_\varepsilon)$ converges to the (to be proved) solution of $(AMSS1)$, which is the right model. We

conjecture that this convergence is true and we can give hints in the next subsection about existence for $(AMSS1)$ which also suggest in which sense this convergence can be true. Returning to $(AMSS_\varepsilon)$, we would like to make clear that it is in fact the right model for what we can numerically implement. Any numerical implementation of $(AMSS1)$ is done on a grid and derivatives of u at a pixel (x,y) computed with the neighbooring pixels. We refer to [AM] where a very easy and most invariant such numerical scheme (due to Luis Alvarez and Frederic Guichard) is proposed for $(AMSS)$. The only alteration which we do for this scheme is following : If (x,y) is a vertex of the grid belonging to $\mathscr{Z}$, we simply fix in the scheme the four pixels surrounding (x,y). In other terms, we call u^n the successive discretized values of u^n and write the Alvarez-Guichard scheme for $(AMSS_\varepsilon)$ in the form

$$u^{n+1}(x,y) = u^n(x,y) + \Delta t F(D^2 u^n(x,y), Du^n(x,y), (x,y)),$$

where of course (x,y) are discrete values and Δt a small enough time (or scale) increment. Then the new scheme, associated with $(AMSS_\varepsilon)$ simply is

$$u^{n+1}(x,y) = u^n(x,y) + \Delta t F(D^2 u^n(x,y), Du^n(x,y), (x,y))$$

if (x,y) are the coordinates of a pixel not touching a $T-junction$, and

$$u^{n+1}(x,y) = u^n(x,y)$$

otherwise. This slight change in the scheme has dramatic consequences in the evolution of the image in scale space, as we shall see in the numerical experiments.

## 5.3   Experiments in junction-preserving image filtering

• **Experiment 3 (two pages). Image filtering preserving Kanizsa singularities on a real image.** First page, u1 : the original image *El caminante*, already analysed in Experiments 1 and 2. Image u2 : junctions of level lines found by the Junction detection algorithm. Image u3 : (AMSS) analysis of u1 at scale $t = 12$. Second page of Experiment 3, Image u4 : u1 smoothed by Algorithm 1 (that is, the same P.D.E. as (AMSS), but with all junctions detected in u2 fixed). Image u5 : all level lines of u3. The structure of the image is lost because junctions are blurred out. Image u6 : level lines of u4, that is, level lines are smoothed but their endpoints on junctions are fixed. The structure of the image is fully preserved (as was already apparent in u4) and the occlusion structure made readable by this topographic map.

u1

u2
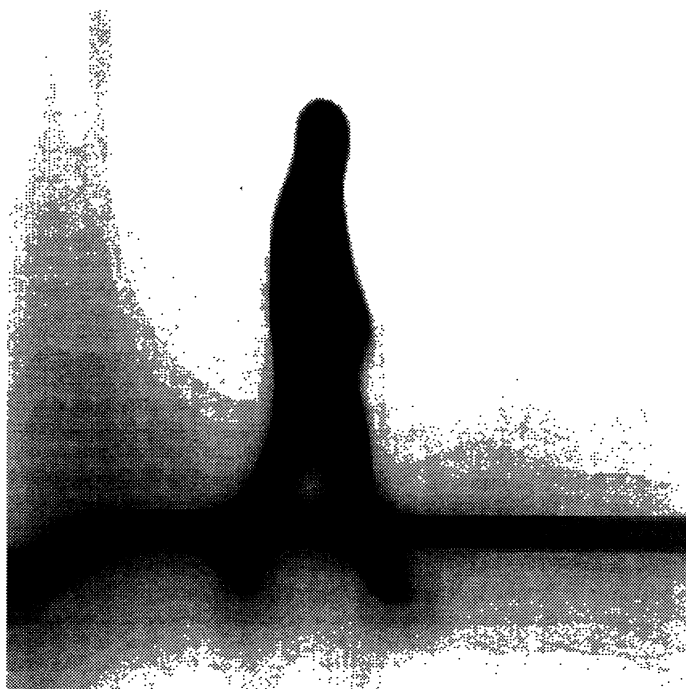
u3

u4

u5

u6

Experiment 3.

5.4 Direct existence proof for the junction preserving smoothing.

We wish to sketch a possible proof for a model related to (AMSS1), but not affine invariant, the Osher-Sethian classical mean curvature. If we do the same adaptation to image analysis as the one yielding (AMSS1), we obtain the equation

$$(AMSS1) \qquad \frac{\partial u}{\partial t} = 1\!\!1_{\mathcal{Z}}(x,y)|Du|(curv(u)), \quad u(0,x) = u_0(x).$$

The corresponding curve evolution model is the so called intrinsic heat equation

$$(IHE1) \qquad \frac{\partial C(t,s)}{\partial t} = curv(C)\vec{n}(t,s), \quad C(t,0) = z_0, C(t,1) = z_1,$$

where z_0, z_1 denote the fixed endpoints of the curve $C(t)$. Equation (IHE1) has existence, uniqueness and regularity results which are proved in [Gr] in the case of an embedded curve without endpoints. In order to generalize Grayson's result to the case where the tips of the curve are fixed, one may proceed as follows. Assuming that the initial curve $C_0(s)$ is parameterized by a parameter s ranging from 0 to 1, we embed C_0 into a periodic curve by setting

$$\tilde{C}(s) = C(0) - C(-s) \quad \text{if} \quad -1 \le s \le 0$$

and then by embedding $\tilde{C}$ into a 2-periodic curve. If, by this process, $\tilde{C}$ has remained a simple curve (a curve without self-intersection), then we can apply the main theorem in [Gr] and assert that $\tilde{C}(t,s)$ is uniquely defined, independent of the initial parameterization, and analytic for every $t > 0$. In addition, because of the uniqueness of the evolution, $\tilde{C}(t,s)$ is equal to the curve obtained by evolving $C_0(-s)$. Thus $\tilde{C}$ is invariant by the symmetry $x \to -x$ in $I\!\!R^2$, so that z_0 belongs to $\tilde{C}$ for every t. In the same way, z_1 belongs to $\tilde{C}$ and we define the solution of (IHE1) as the part of $\tilde{C}$ joining z_0 and z_1. In the case where $\tilde{C}_0$ does present self-intersections, we conjecture that the Grayson proof applies anyway, since the self-intersections happen between parts of the curve belonging to different periods and cannot create singularities. It is therefore very likely that these self-intersections disappear after a while and the curve tends to a straight line joining z_0 and z_1 as $t \to \infty$. We do the same conjecture for the equation

$$(ASS1) \qquad \frac{\partial C}{\partial t} = (curv(C))^{\frac{1}{3}}\vec{n}(t,s), \quad C(t,0) = z_0, C(t,1) = z_1,$$

with the difference that the convergence to the straight line should take a finite time.

REFERENCES

[AGLM1] L. Alvarez, F. Guichard, P.L. Lions and J.M. Morel , Axioms and fundamental equations of image processing Report 9216, 1992 CEREMADE. Université Paris Dauphine . Arch. for Rat. Mech. 16, IX, 200-257, 1993

[AM1] L. Alvarez and J.M. Morel. Formalization and Computational Aspects of Image Analysis, Acta Numerica, 1994, Cambridge University Press.

[AM] L. Alvarez and Freya Morales. Affine Morphological Multiscale Analysis of Corners and Multiple Junctions. Ref 9402, August 1994, Dept. Informatica y Systemas, Universidad de Las Palmas de Gran Canaria. To appear in International Journal of Computer Vision.

[BMO] B. Merriman, J. Bence and S.Osher, Motion of multiple junctions : a level set approach, CAM Report 93-19. Depart. of Mathematics. University of California, Los Angeles CA, June 1993.

[CCCD] V. Caselles, F. Catté, T. Coll and F. Dibos. A geometric model for active contours in image processing. Numerische Mathematik, 66, 1-31, 1993.

[CCM] V. Caselles, T. Coll and J.M. Morel. A Kanizsa programme, preprint, Ceremade, 1995. Submitted to Int. Journal of Comp. Vision.

[CGG] Y.G. Chen, Y. Giga and S. Goto. Uniqueness and existence of viscosity solutions of generalized mean curvature flow equations. J. Diff. Geometry, 33, 749-786, 1991.

[CIL] M.G. Crandall, H. Ishii and P.L. Lions , User's guide to viscosity solutions of second order partial differential equation, Bull. Amer. Math. Soc., 27, 1-67, 1992.

[ES] L. C. Evans and J. Spruck. Motion of level sets by mean curvature. J. Differential Geom., (33): 635-681, 1991.

[F] W. Fuchs. Experimentelle Untersuchungen ueber das simultane Hintereinandersehen auf der selben Sehrichtung, Zeitschrift fuer Psychologie, 91, 154-253, 1923

[GH] M. Gage and R.S. Hamilton , The heat equation shrinking convex plane curves, J. Differential Geometry **23**, 69–96, 1986.

[GGIS] Y. Giga, S. Goto, H. Ishii and M.M. Sato. Comparison principle and convexity preserving properties for singular degenerate parabolic equations on unbounded domains. Indiana Univ. Math. J., 40, 443-470, 1991.

[Gr] M. Grayson, The heat equation shrinks embedded plane curves to round points, J. Differential Geometry **26**, 285–314, 1987.

[GM] F. Guichard and J.M. Morel. Image Iterative Smoothing and P.D.E.'s. To appear, Cambridge University Press.

[Ka] G. Kanizsa *Vedere e pensare*, Il Mulino, Bologna, 1991.

[KTZ] B.B. Kimia, A. Tannenbaum, and S.W. Zucker , On the evolution of curves via a function of curvature, 1: the classical case, J. of Math. Analysis and Applications **163**, No 2, 1992.

[MS] J.M. Morel and S. Solimini. *Variational methods in image processing*, Birkhäuser, 1994.

[NM] M. Nitzberg and D. Mumford. "The 2.1 Sketch", in Proceedings of the Third International Conference on Computer Vision, Osaka 1990.

[OS] S. Osher and J. Sethian, Fronts propagating with curvature dependent speed: algorithms based on the Hamilton-Jacobi formulation, J. Comp. Physics **79**, 12–49,

1988.

[ST1] G. Sapiro and A. Tannenbaum. On affine plane curve evolution. Journal of Functional Analysis, 119, 1, 79-120, 1994.

[Wi] A.P. Witkin. Scale-space filtering. Proc. of IJCAI, Karlsruhe 1983, 1019-1021.